Systematic study of light-induced effects in hydrogenated amorphous silicon

K. Zellama, H. Labidi, P. Germain, and H. J. von Bardeleben
Groupe de Physique des Solides, Université Paris VII, 2 place Jussieu, 75251 Paris CEDEX 05, France

L. Chahed* and M. L. Theye
Laboratoire d'Optique des Solides, Université Paris VI, 4 place Jussieu, 75252 Paris CEDEX 05, France

P. Roca i Cabarrocas and C. Godet
Laboratoire de Physique des Interfaces et des Couches Minces, Ecole Polytechnique, 91128 Palaiseau, France

J. P. Stoquert
IN2P3, Centre de Recherches Nucléaires, Laboratoire de Physique et Application des Semiconducteurs, Boîte Postale 20, 67037 Strasbourg CEDEX, France
(Received 7 October 1991)

A systematic investigation of the origin of the photoinduced changes in the defect density of states in the pseudogap of undoped hydrogenated amorphous silicon (*a*-Si:H) has been carried out on films deposited by glow-discharge decomposition of silane under different conditions. We used several complementary techniques, such as junction capacitance versus temperature, electrical conductivity, electron-spin resonance, and photothermal deflection spectroscopy, to determine the shifts in the Fermi-level (E_F) position as well as the variation of the defect density of states, within the forbidden gap, after annealing (state *A*) and light-soaking (state *B*) treatments. The total hydrogen concentration and the hydrogen bonding configurations of each sample were analyzed by elastic-recoil-detection analysis (ERDA) and infrared (ir) transmission measurements, respectively, both for state *A* and state *B*. The experimental results show in all cases an increase in the bulk density of states accompanied by a shift of E_F towards the valence band in the light-soaked state *B* with respect to the annealed state *A*, but these changes depend considerably on the deposition conditions of the films. On the other hand, no change is detected either in the ERDA or in the ir spectra. Moreover, it is found that when the saturated light-soaked samples are partially annealed at temperatures ranging from 110 °C to 130 °C and for times less than 15 min, and then left in the dark at room temperature for 24 h and more, a long-time process, characterized by a variation of the density of states as well as by a motion of E_F within the gap, occurs in these films. The observed behavior is completely different from one sample to another. From the analysis of the results, it is suggested that in some samples the photodegradation is mainly due to a trapping of the excess free carriers at charged spinless defects, which must be present in the sample at equilibrium in addition to the neutral dangling bonds.

I. INTRODUCTION

One of the most intriguing properties of hydrogenated amorphous silicon (*a*-Si:H) is the so called Staebler-Wronski (SW) effect.[1,2] These authors reported a large decrease in the dark conductivity measured at room temperature by about 3 orders of magnitude after prolonged illumination of *a*-Si:H films. A decrease of the photoconductivity by about 1 order of magnitude was simultaneously observed. This behavior is directly related to the creation of defects, accompanied by a shift of the Fermi level within the gap of the amorphous material, due to illumination.[1,2] These defects are found to be metastable because they can be eliminated by a simple annealing at temperatures between 150 °C and 200 °C.

Since this pioneer work, a large number of studies have been carried out on the SW effect. They clearly indicate that the observed metastable photoinduced effects, which strongly affect the electronic and optical properties of *a*-Si:H,[3–15] correspond to a real change in the bulk properties of the films, even if some surface or interface effects may be present.[2,13–21] However, their origin is not yet fully clarified.

Several models have been proposed to explain the SW effect. The first one suggests that the reversible light-induced changes in the density of the neutral dangling bonds D^0 result from the breaking of the weak Si-Si bonds through a nonradiative recombination of the photoinduced carriers on these bonds.[5,14,15] The hydrogen can play an important role in this process.[5,14,15,22] A second model assumes a simple trapping of the excess carriers at charged defects already existing in the material at equilibrium in addition to the neutral dangling bonds, such as the T_3^+-T_3^- pair centers.[23–25] These T_3^+-T_3^- pairs are characterized by a negative correlation energy *U*. The conversion of these charged defects into neutral ones results in an increase of the spin density upon illumination. In this case also, the hydrogen might play a role through a possible relaxation of the configuration of these defects.[23–26] In a more recent

work, the increase of the density of neutral dangling bonds after light exposure has been interpreted as rather due to the breaking of weak Si-H bonds, in particular at sites such as Si-H-Si three-center bonds.[27] Another model suggesting that the two hydrogen-atom complexes, denoted by H_2^* molecules, play a predominant role in the SW effect, has been also proposed.[28,29] It is important to notice that, in all these models, the hydrogen seems to be directly involved in the mechanisms of the apparition of the metastable light-induced defects.

In order to obtain more details on the microscopic processes of defect creation due to illumination, and also to better understand the role played by hydrogen in these mechanisms, we have performed extensive studies on *a*-Si:H deposited by the glow discharge technique at different substrate temperatures, which therefore present different hydrogen content. Several complementary measurements, namely, capacitance versus temperature (*C-T*), electrical conductivity, electron-spin resonance (ESR), photothermal deflection spectroscopy (PDS), infrared (ir), and elastic-recoil-detection analysis (ERDA), were first carried out on simultaneously deposited samples both in their full dark annealed state (state *A*) and in their saturated light-soaked state (state *B*).

In addition, a second set of experiments, restricted to *C-T* measurements correlated with electrical conductivity and ESR measurements, was performed on the same samples after partial annealing, starting from state *B*, at temperatures not exceeding 130 °C and for times ranging from 10 to 15 min. The same measurements were then repeated after the samples were left in the dark at room temperature in this partially annealed state for periods longer than 24 h.

The new results obtained for the partially annealed samples confirm that more than one type of defects has to be considered in order to fully understand the origin of the metastable light-induced changes in *a*-Si:H.

II. EXPERIMENTAL CONSIDERATIONS

Undoped *a*-Si:H samples were deposited by rf glow-discharge (GD) decomposition of pure silane under optimized plasma conditions: rf power of 0.1 W/cm^2, silane flow rate of a total gas pressure of 50 m Torr, at three different substrate temperatures $T_s = 100$, 150, and 250 °C; they are labeled series 1, 2, and 3, respectively. In each run, several samples are deposited simultaneously on p^+-type crystalline silicon and indium-tin-oxide (ITO) substrates for the *C-T* and ERDA experiments, undoped single-crystal silicon for ir measurements, and quartz substrates for ESR, PDS, and conductivity experiments. For each series, two sets of samples with different thicknesses ranging from 1 to 4.64 mm, obtained in two different runs, were investigated (see Table I). The deposition conditions along with the average hydrogen concentration C_H as measured by ERDA for the three series are summarized in Table I. The measured optical gap E_{04}, defined as the energy at which the absorption coefficient α is equal to 10^4 cm^{-1}, is also presented in the same table.

We obtain the state *A* after annealing each sample at 200 °C for 20 min under a vacuum of 10^{-6} Torr. State *B* is reached by exposing the films to white light at an average power of 1 W/cm^2 supplied by a xenon arc lamp for 16–20 h at room temperature. To avoid the heating of the samples during light exposure, we used a water filter to eliminate the ir radiation. We checked that the temperature of the films did not exceed 35 °C during illumination by using a thermocouple attached near the sample and receiving the same illumination. The partially annealed state is obtained by heating each sample in state *B* at temperatures ranging from 110 °C to 130 °C, for 10–15 min under vacuum or He atmosphere. As previously described in detail,[30–32] the *C-T* experiments are performed on Schottky barrier configurations realized by depositing a semitransparent top platinum layer of about 100 Å thick and 1.2 mm in diameter on the surface of the *a*-Si:H film. We measure the variation of the capacitance C and of the conductance G/ω of the diode as a function of the temperature in the 200–400-K range at different frequencies ω varying from 5 Hz to 1 kHz. From the *C-T* curves, we calculate the quantity $C^2(dC/dT)^{-1}$ which can be written as follows:[32,33]

$$C^2(dC/dT)^{-1} = A\,[\varepsilon q g(E_F)]^{1/2}T + aT^2 + bT^3 + \cdots ,$$

where A, ε, and q are, respectively, the area of the Schottky diode, the *a*-Si:H static dielectric constant, and the electron charge. The quantity $g(E_F)$ represents the density of states at E_F. We can also deduce from these measurements the position of E_F in the pseudogap, as explained in the following section. The electrical conductivity measurements are carried out in coplanar configuration with platinum electrodes 4 mm apart, the sample being mounted in a quartz tube evacuated to 10^{-6} Torr.

The ESR spectra are obtained at room temperature using an ESR *X*-band spectrometer at 9.36 GHz. We deduce the concentration of spins Ns (i.e., neutral dangling bonds D^0) from the ESR signal corresponding to a g factor of 2.0055. The estimated uncertainly on the Ns absolute values is of the order of 50%.

The PDS experiments are carried out over a large spectral range, from 2 down to 0.6 eV, using a stabilized quartz iodine lamp (24 V, 250 W) followed by a Jobin

TABLE I. Deposition conditions of the *a*-Si:H films (series 1–3) along with the values of the optical gap (E_{04}) and the total H concentration.

Series	$T_{substrate}$ (°C)	Thickness (μm)	Pressure (m Torr)	rf power (W/cm^2)	H concent. (at. %)	E_{04} (eV)
1	100	3.5, 4.64	50	0.1	16±1	1.93±0.01
2	150	1, 3.74	50	0.1	12±1	1.92±0.01
3	250	3.5, 4.64	50	0.1	6±1	1.88±0.01

Yvon H 25 monochromator as the exciting beam, and a 1-mW He-Ne laser as the probe beam. The chopping frequency is 13 Hz and the samples are immersed in CCl_4. Under such experimental conditions of thermally thin samples, the PDS signal is simply proportional to the film absorptance $A=1-(R+T)$. The PDS spectra are calibrated by fitting to the absorptance curves calculated in the high absorption range ($\alpha \geq 10^3$ cm^{-1}) with the complex refractive index and film thickness deduced as usually from transmittance measurements. The absorption coefficient α is then determined via appropriate thin-film expressions.[34] The absorption coefficient spectra over the whole spectral range are obtained by combining the optical and PDS results. From these spectra, we deduce the optical gap E_{04}, the inverse slope of the exponential part of the edge (Urbach energy) E_0 which is considered as a parameter characteristic of disorder, and a number N_D standing for the "optical" integrated defect state density. N_D is determined from the subgap optical absorption after substraction of the tail states contribution according to the widely used calibration procedure;[35] although the absolute N_D values may be questioned, this method of evaluation of the total defect state density is fully justified in the present comparative studies, where we are essentially interested in changes of this density for the same sample. The values of α at, say, 1.15 eV, would provide similar information, but values of the total density of states are easier to handle for our purpose.

The ir transmission spectra are obtained using a Perkin Elmer 580 B spectrometer over the 400–2500-cm^{-1} wave-number range, which allows us to observe the different vibrational modes (stretching, bending, and wagging) of the Si-H bonds.

III. RESULTS

We present first the results obtained for the full dark annealed state (A) and the saturated light-soaked state (B). In a second subsection, we will discuss the results relative to the partial annealing and long-time evolution experiments.

A. Comparison between the full dark annealed state (A) and the saturated light-soaked state (B)

We report in Fig. 1 typical C-T results obtained for the samples of series 3 in states A and B. The corresponding calculated quantity $C^2(dC/dT)^{-1}$ is plotted as a function of T in Fig. 2. The slopes of the straight lines in this figure provide the density of states at E_F, $g(E_F)$, in states A and B. An Arrhenius plot of the logarithm of the frequency ω vs the inverse of the temperature values corresponding to the intercepts of these lines with the temperature axis gives the activation energy of the bulk conductivity E_σ.[33] The values obtained for $g(E_F)$ and E_σ for all the series (1–3) in their states A and B are presented in Table II.

We observe in all cases an increase in E_σ, which corresponds to a shift of E_F towards the valence band ("direct" SW effect), as well as an increase in $g(E_F)$, when going from state A to state B. But, contrary to what we are expecting from the results of a previous study,[30] the largest shift in the E_F position as well as the largest change in $g(E_F)$ is obtained for series 3 deposited at the highest substrate temperature (i.e., containing the lowest H concentration). For clarity, we report in Table II for the three series the ratios of the density of states at E_F in state B and state A $g_B(E_F)/g_A(E_F)$ and the values of the shift of the Fermi level $\Delta E_F = E_{\sigma B} - E_{\sigma A}$, taken as positive when E_F moves towards the valence band. The behavior observed for E_σ is confirmed by the results obtained for the $(E_C$-$E_F)$ quantity deduced from the temperature dependence of the dark electrical conductivity (σ_{RT}) obtained from the coplanar conductivity measurements, which show that the largest increase in the $(E_C$-$E_F)$ values is also observed for series 3. Moreover, the $(E_C$-$E_F)$ values measured in state A are lower for the samples exhibiting the lowest hydrogen concentration, in agreement with the results obtained for E_σ. On the other hand, the coplanar electrical conductivity results indicate that the room-temperature value of the dark conductivity σ_{RT}, measured in state A, is also significantly higher (by about 3 orders of magnitude) for series 3, deposited at the

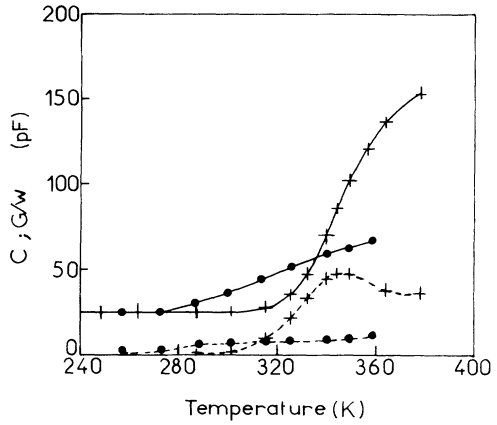

FIG. 1. Typical variation of C (solid line) and G/ω (dashed line) vs temperature obtained from the C-T experiments for series 3 at 200 Hz in ●, state A; and +, state B.

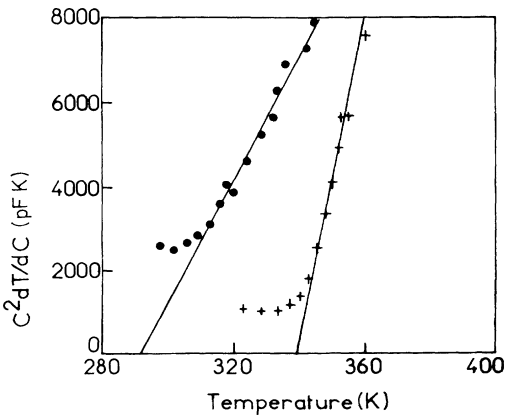

FIG. 2. Plot of the quantity $C^2(dC/dT)^{-1}$ vs temperature corresponding to the results presented in Fig. 1 for series 3 in ●, state A; and +, state B.

TABLE II. Values of the density of states at the Fermi level $g(E_F)$ and of E_σ (i.e., the E_F position with respect to the conduction mobility edge E_C) deduced from the C-T experiments, along with the values of $(E_C$-$E_F)$ and σ_{RT} deduced from the conductivity measurements for all the film series (1–3) in states A and B. We also present, for clarity, the values of the ratio $g_B(E_F)/g_A(E_F)$ and $\Delta E_F = E_{\sigma B} - E_{\sigma A}$ (shift of E_F when going from state A to state B).

Series	$T_{substrate}$ (°C)	H concent. (at. %)	σ_{RT} $[(\Omega\,cm)^{-1}]$ State		$g(E_F)$ (10^{15} $cm^{-3}eV^{-1}$) State		$\frac{g_B(E_F)}{g_A(E_F)}$	E_σ (eV) State		$\Delta E_F = E_{\sigma B} - E_{\sigma A}$ (eV)	E_C-E_F (eV) State	
			A	B	A	B		A	B		A	B
1	100	16	9×10^{-10}	2.3×10^{-11}	6.6	14.5	2.2	0.83	0.92	0.09	0.8	0.88
2	150	12	1.1×10^{-10}	1.6×10^{-12}	0.8	6.6	8.2	0.8	0.95	0.15	0.8	0.97
3	250	6	2.8×10^{-7}	7.5×10^{-11}	1.2	15	14	0.65	0.94	0.29	0.6	0.96

highest substrate temperature, than for series 1 and 2, deposited at lower temperatures. After light exposure, σ_{RT} decreases for all the samples, as commonly observed. We obtain a decrease in σ_{RT} by up to 3 orders of magnitude with respect to the annealed state A. The values of σ_{RT} and $(E_C$-$E_F)$ measured in the full dark annealed state and the saturated light-soaked state for series 1–3 are summarized in Table II. We present in Fig. 3 typical data for the dark conductivity variation as a function of reciprocal temperature $\sigma(T^{-1})$, deduced from the coplanar electrical conductivity experiments for series 3 in the as-deposited state and in states A and B. These data show that the as-deposited state is lying between state A and state B, with intermediate values for both $(E_C$-$E_F)$ and σ_{RT}.

Concerning the PDS and ESR results, we observe the same behavior for the "optical" integrated defect state density N_D and the spin density N_s (i.e., the density of neutral dangling bonds D^0). In state A, both N_D and N_s are higher when the samples exhibit a higher H content. Upon illumination, both N_D and N_s increase for all the samples. However, contrary to the C-T and $\sigma(T)$ results, the largest changes in N_D and N_s are observed for series 1 deposited at the lowest substrate temperature. This apparent contradiction will be discussed in detail in Sec. IV.

Like the defect density (N_D or N_s), the Urbach energy E_0 in state A takes the largest value for the samples deposited at the lowest temperature (i.e., with the highest H content), which means that these samples exhibit more disorder. After light exposure, E_0 stays almost constant for series 2 and 3, it increases by about 3 meV for series 1. This last observation might indicate an increase of the disorder due to illumination in this series. But the apparent E_0 change can also reflect the increasing contribution of the defect related absorption in the Urbach edge region. We summarize in Table III the results obtained for E_0, N_D, and N_s in states A and B for all the series. We also report in this table, for comparison, the ratios N_{DB}/N_{DA} and N_{sB}/N_{sA} for series 1–3. We present in Figs. 4(a)–4(c) typical optical absorption coefficient spectra $\alpha(E)$ as deduced from the optical and PDS experiments in both states A and B for series 1, 2, and 3, respectively. It may be important to notice that the spectrum of Fig. 4(b) corresponding to series 2 in state A exhibits an additional shoulder centered at about 1.4 eV, which does not appear in the corresponding spectra for series 1 and 3. This probably means that additional shallow defect states are initially present in series 2. Such defect states do not seem to exist in series 3; in series 1, if they exist they cannot be distinguished from the deep defect states.

Typical ir spectra obtained for series 1 and 3 are reported in Fig. 5 for state A. They indicate that hydrogen is mostly present in the Si-H configuration characterized by the stretching vibrational mode peak centered at 2000 cm^{-1} and the wagging vibrational mode peak centered at 650 cm^{-1}. A few $Si\text{-}H_2$ complexes characterized by a broadening of the stretching mode peak in the 2090-cm^{-1} range, and the apparition of a bending vibrational mode peak centered at 890 cm^{-1}, may also be present in the films deposited at the lowest substrate temperature (100 °C). The proportion of the $Si\text{-}H_2$ complexes decreases as the temperature of deposition increases and eventually disappears for the samples deposited at 250 °C. Upon illumination, we do not observe, within experimental uncertainties, any change, either in the position, or in

TABLE III. Values of the integrated optical density of defect states N_D and of the Urbach parameter E_0 deduced from the PDS experiments and of the density of spins N_s deduced from the ESR measurements in states A and B for all the film series (1–3). We also present the ratios N_{DB}/N_{DA} and N_{sB}/N_{sA}.

Series	$T_{substrate}$ (°C)	PDS results N_D(10^{16} cm^{-3}) State A	State B	E_0 (meV) State A	State B	N_{DB}/N_{DA}	ESR results N_s(10^{16} cm^{-3}) State A	State B	N_{sB}/N_{sA}
1	100	1.3	6	55.5	58.5	4.62	2.5	10.8	4.3
2	150	0.46	1.3	51.3	51.8	2.83	1.5	5.1	3.4
3	250	0.51	1.5	51	50.9	2.95	0.9	2.9	3.2

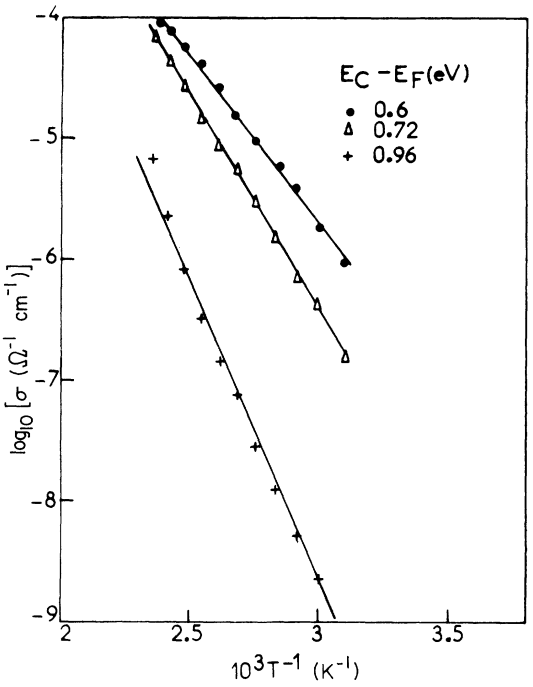

FIG. 3. Typical variation of $\log_{10}\sigma$ vs the inverse of temperature for series 3 in △, as-deposited state; ●, state A; and +, state B.

the intensity of the different peaks, in agreement with our previous ir results.[30] This indicates that light exposure does not induce any structural modification in the bonded hydrogen configurations which can be detected with the sensitivity of the ir absorption measurements.

Furthermore, we checked by ERDA for series 1, which exhibits the highest hydrogen content, that the total H concentration did not vary after illumination. This in agreement with the fact that the optical gap E_{04} remains constant when going from state A to state B, for all the samples.

B. Experimental results obtained after partial annealing and long-time evolution

Starting from the saturated light-soaked state (B), the samples of each series 1–3 are partially annealed in the dark at temperatures ranging from 110 °C to 130 °C for 10–15 min, i.e., without reaching in any case the full dark annealed state A. The results obtained from the C-T, electrical dark conductivity, and ESR experiments carried out on these samples just after such a partial annealing, show that they reach, as expected, an intermediate state A_1, lying between states B and A, characterized by a shift of the E_F position towards the conduction band accompanied by a decrease in the density of states at E_F $g(E_F)$ as well as in the density of spins N_s. The amplitude of these changes depends on the deposition temperature of the sample. It is also found that annealing at temperatures lower than 100 °C does not produce any effect with respect to the state B.

Quite surprising results are obtained when the same experiments are carried out again on the samples, after they were left in state A_1 in the dark at room temperature under vacuum or He atmosphere, for periods longer than 24 h. We observe a completely different behavior for series 3 as compared to series 1 and 2. Samples of series 3 deposited at the highest substrate temperature (250 °C) reach a state B_1 intermediate between state A_1 and state B, characterized by a backward shift of E_F towards the valence band and a relative increase of $g(E_F)$ with

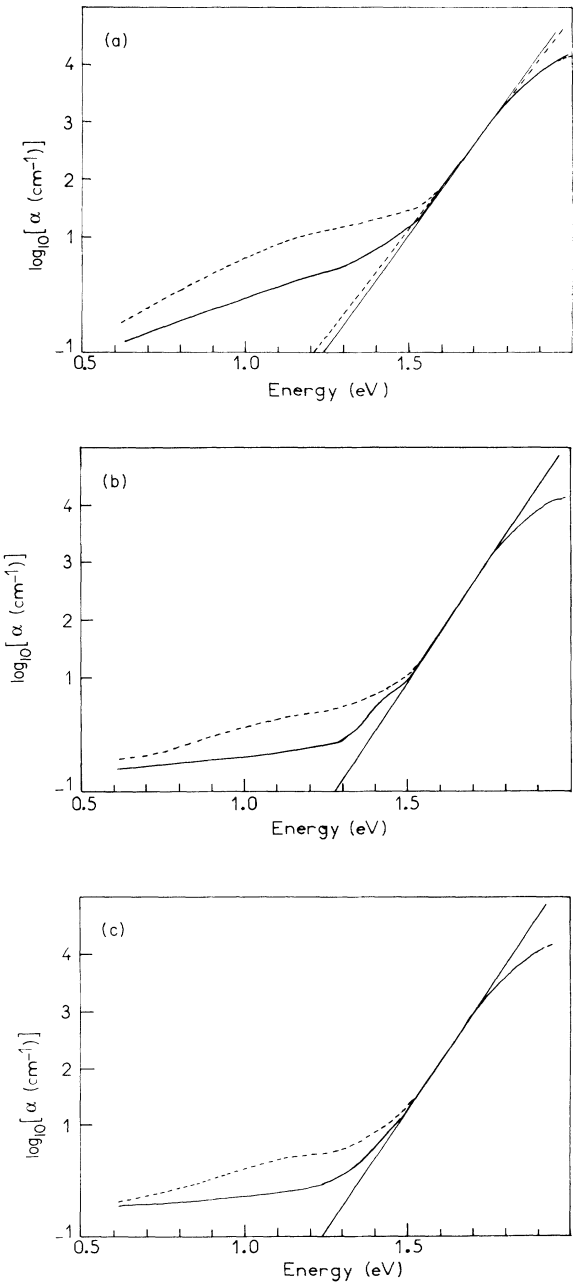

FIG. 4. Typical variation of the optical absorption coefficient α as a function of energy in state A (solid line) and state B (dashed line) for (a) series 1, (b) series 2, and (c) series 3.

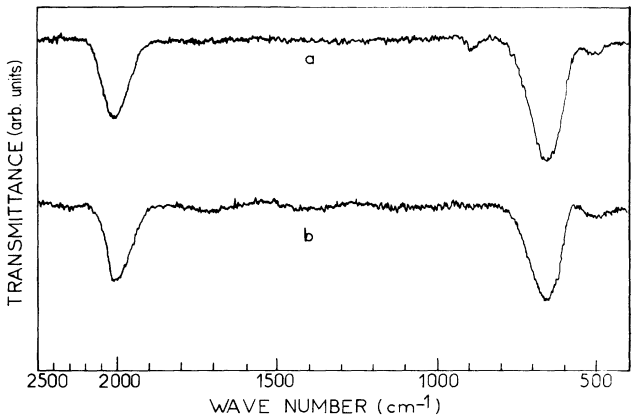

FIG. 5. Comparison of the ir transmission spectra obtained in state A for (a) series 1 and (b) series 3.

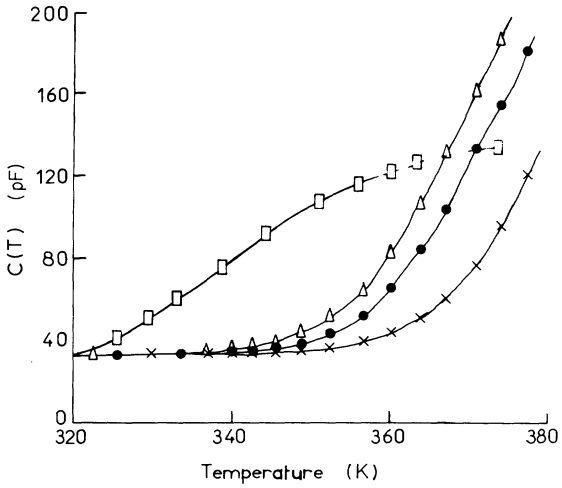

FIG. 6. Typical variation of the capacitance C vs temperature obtained for series 1 at 40 Hz in □, state A; ×, state B; ●, state A_1 (after annealing at 130 °C for 15 min); and △, state A_2 (reached from state A_1 after 48 h in the dark at room temperature).

respect to state A_1. On the other hand, samples of both series 1 and 2 deposited at lower temperatures (100 and 150 °C, respectively) reach a state A_2 intermediate between state A_1 and state A, for which the Fermi level E_F has moved further towards the conduction band, by almost the same amount for series 1 and series 2. Only a small decrease in $g(E_F)$ is observed for both series. An important point is that we did not detect any change in the spin density N_s with respect to state A_1 either for series 1 and 2 (state A_2), or for series 3 (state B_1), suggesting that the long-time process does not affect the neutral dangling bond density. Finally, it is worth noticing that, for times longer than 60 h, no significant change with respect to both states B_1 and A_2 is detected: $g(E_F)$, E_σ, and N_s stay almost constant. The C-T and ESR results obtained for the different series in states B, A_1, and B_1 or state A_2 are summarized in Table IV. We report in Figs. 6 and 7, typical C-T curves corresponding to states A and B, to state A_1 obtained after partial annealing at 130 °C for 15 min and to the state reached from state A_1 after 48 h in the dark at room temperature, for series 1 and 3, respectively.

IV. DISCUSSION

It is important to point out at this stage that, as indicated in Sec. II, we have studied two sets of samples in the three series (1–3), and that the experimental results we reported in this study, which were carefully checked by repeating the measurements, correspond to the typical behavior of each series. Indeed, the results were found to be perfectly reproducible within each series.

The PDS and ESR results obtained for states A and B summarized in Table III indicate that series 1 containing the highest hydrogen concentration (16 at. %) exhibits the largest increase in the integrated "optical" defect density (N_D) as well as in the density of neutral dangling bonds D^0 (N_s) after light exposure. These changes are less important, and about the same for N_D on the one hand and N_s on the other hand, for series 2 and 3 depos-

TABLE IV. Values of $g(E_F)$ and E_σ deduced from the C-T measurements and N_s deduced from the ESR experiments for all the film series (1–3) in state B, state A_1 (reached after partial annealing at 130 °C for 15 min), and state A_2 or B_1 (reached from state A_1, after the films were left in state A_1 in the dark at room temperature for 48 h and more).

Series		Experiments	State B	State A_1	State B_1 or A_2 48 h	60 h	127 h	8 days
1	C-T	E_σ (eV)	0.92	0.87	0.85 A_2			
		$g(E_F)$ (10^{15} cm^{-3}eV^{-1})	14.5	9	8 A_2			
	ESR	N_s(10^{16} cm^{-3})	10.8	7.8	7.7	7.6	7.6	
2	C-T	E_σ (eV)	0.95	0.89	0.86 A_2			
		$g(E_F)$ (10^{15} cm^{-3}eV^{-1})	6.6	2	1.4 A_2			
	ESR	N_s(10^{16} cm^{-3})	5.1	2.9	2.9	2.9	2.8	2.8
3	C-T	E_σ (eV)	0.94	0.72	0.8 B_1	0.85	0.86	
		$g(E_F)$ (10^{15} cm^{-3}eV^{-1})	15	6.9	8 B_1	8.3	8.3	
	ESR	N_s (10^{16} cm^{-3})	2.9	2.1	2.1	2.1	2.1	2.1

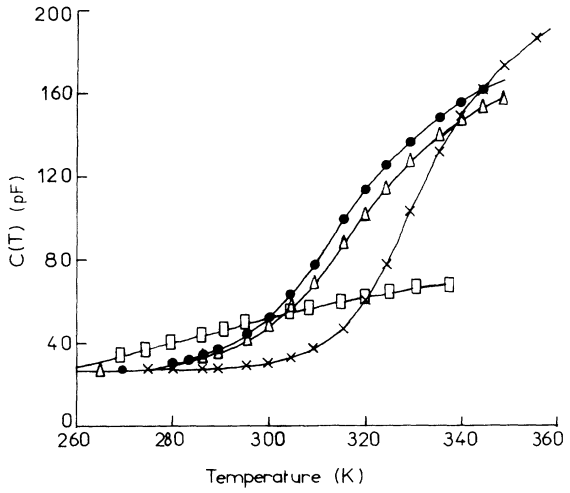

FIG. 7. Typical variation of C vs temperature obtained for series 3 at 20 Hz in □, state A, ×, state B; ●, state A_1 (after annealing at 130°C for 15 min); and △, state B_1 (reached from state A_1 after 48 h in the dark at room temperature).

ited at higher substrate temperature (i.e., with lower hydrogen concentration). As for the C-T and electrical conductivity results reported in Table II for states A and B, they show that the shift of E_F towards the valence band upon illumination is more important for series 3 ($\Delta E_F \sim 0.29$ eV) deposited at the highest substrate temperature, than for series 1 ($\Delta E_F \sim 0.09$ eV) and series 2 ($\Delta E_F \sim 0.15$ eV) deposited at lower temperature. The same trend is observed for the density of states at E_F, $g(E_F)$; the largest ratio $g_B(E_F)/g_A(E_F)$ is also obtained for series 3 [$g_B(E_F)/g_A(E_F) \sim 14$], compared to series 1 and series 2 for which $g_B(E_F)/g_A(E_F)$ is equal to 2.2 and 8.2, respectively.

This apparent contradiction between the C-T results and the PDS and ESR ones could be explained by the fact that the new light-induced defect states may have different energy distribution in the three sample series. We consider here another interpretation relying on the assumption of the existence of charged defects, such as the T_3^+-T_3^- pair centers,[23–25] in addition to neutral dangling bonds, in which the shift of the Fermi level can only be due to a change in the occupation of the defect states.

If we apply this simple rule to series 1, which presents in state A the highest total defect density N_D, we can predict only a slight shift of E_F within the gap, which is effectively observed ($\Delta E_F \sim 0.09$ eV). The fact that, after illumination, we obtained a small ratio $g_B(E_F)/g_A(E_F)$ (~ 2.2) leads us to think that the large increase in N_D and N_s corresponds to defect states distributed not only in the midgap region, but also closer to the band edges (which would explain that E_0 increases when going from state A to state B). This increase is not, however, large enough to induce a large shift of E_F which is already pinned at midgap due to the high density of defects existing in state A. For series 3, which exhibits in state A a much lower defect density than series 1, we observe on the contrary a large shift of E_F within the gap ($\Delta E_F \sim 0.29$ eV), as expected by the application of the same rule. The large increase in $g(E_F)$ due to illumination, with only a minor concomitant change in N_s and N_D, suggests a modification of the energy distribution of the defect states at midgap as well as below the E_F position in state A. Series 2, which has also a low defect state density in state A, presents only a moderate shift of E_F ($\Delta E_F \sim 0.15$ eV) after illumination but the relatively large increase in $g(E_F)$ [$g_B(E_F)/g_A(E_F) \sim 8.2$] for a nearby position of E_F leads us to conclude that most of the photoinduced defects are neutral dangling bonds giving states in the middle of the gap. One must recall that there are probably additional defects present in state A in this series which do not appear in series 1 and 3, as evidenced by the PDS results.

Let us now discuss the whole experimental results obtained for series 1–3 in the full dark annealed state and the light-soaked state in the context of the different models proposed to explain the SW effect.

The increase in $g(E_F)$ and N_s observed for series 1 and 2 after light exposure can be explained by the bond-breaking model[5,14,15,22] as well as by the model proposed by Adler[23–25] which, as already emphasized, assumes the existence in the amorphous material of charged dangling bonds such as the T_3^+-T_3^- pair centers in addition to the traditional neutral dangling bonds D^0. Nevertheless, the large shift in the E_F position upon illumination observed for series 3, with only a minor concomitant change in N_s and N_D, can be better understood by a simple trapping of the photogenerated free carriers on the charged T_3^+-T_3^- pair defects.

As it has been presented in detail in previous studies,[23–25] these charged centers, which are more efficient traps for the carriers than the neutral ones, should be present at equilibrium in the films. Depending on whether the T_3^+ and T_3^- centers are located in relatively unstrained or strained regions, i.e., regions in which atomic relaxations can freely occur or not, we might have the following reactions:

$$\begin{aligned} &T_3^+ + e^- \rightarrow T_{sp^2}{}^0 \rightarrow D^0 \ , \\ &\qquad\quad\ \updownarrow \\ &T_3^- + h^+ \rightarrow T_p{}^0 \rightarrow D^0 \ . \end{aligned} \tag{1}$$

The neutral donor state $T_{sp^2}{}^0$ (or acceptor state $T_p{}^0$) has the possibility either to release the trapped carrier or to become a D^0 center by changing its hybridization into sp^3, or to convert into the opposite state ($T_{sp^2}{}^0 \leftrightarrow T_p{}^0$). These different reactions are governed by precise conditions.[23–25,36,37]

Taking into account the mass action law, the concentration of the T_3^+-T_3^- pair separated by a distance R is given by the expression[24]

$$C_{T_3^+\text{-}T_3^-}(R) = C_{T_c^+\text{-}T_3^-}(\infty)\exp(e^2/2\varepsilon R k T_s) \ , \tag{2}$$

where $C_{T_3^+\text{-}T_3^-}(\infty)$ is the pair concentration at large separations and e, ε, T_s, and k are, respectively, the electron charge, the effective dielectric constant, the deposition temperature, and the Boltzmann constant.

It has been suggested[24] that the spatially close T_3^+-T_3^- pairs, which must represent the majority of charged gap states, correspond to gap states respectively close to the conduction- and the valence-band mobility edges, and are deeply involved in the motion of the Fermi level within the gap upon illumination. As a matter of fact, depending on the relative concentration of the T_3^+ and T_3^- centers after light exposure, the shift of E_F will be more or less important and either positive or negative (i.e., either towards the valence band or towards the conduction band[30]). On the contrary, the widely separated T_3^+-T_3^- pairs introduce states closer to midgap, and are not likely to release their trapped carriers very rapidly. When such a pair captures an electron (or hole), it transforms rapidly into D^0-T_3^- (T_3^+-D^0) pairs, then when the remaining charged site captures a free carrier, this results in the apparition of additional widely separated neutral D^0-D^0 pairs detectable by ESR. We can reasonably admit that the close T_3^+-T_3^- pairs play a predominant role in the effects which we observed in series 3, deposited at the highest substrate temperature, when going from state A to state B, while the results obtained for series 1 deposited at the lowest substrate temperature, for the same $A \rightarrow B$ transition, are more indebted to the widely separated T_3^+-T_3^- pairs. Let us now go further into the discussion by considering the results obtained after the partial annealing and the long-time evolution, which are summarized in Table IV.

We must first point out that the observed effects cannot be related to equilibration phenomena. As a matter of fact, even if we consider that the equilibration temperature T_E of the a-Si:H film in state B may be lower than that in state A because of the new defect state distribution,[38] the fact that T_E is about 180 °C for the undoped material[39] and 80–130 °C for the doped a-Si:H samples[40] which have defect concentrations higher by about 2 orders of magnitude, leads us to the reasonable assumption that T_E, for intrinsic a-Si:H in state B is in any case higher than 130 °C, which is the maximum value used in the partial annealing experiments. If now we turn to the changes with time observed in series 1–3 after partial annealing, we find that they are easier to understand in the framework of the "charge distribution" model.[23–25]

Indeed, since we observe a direct SW effect (i.e., a shift of E_F towards the valence band) for all the samples when going from the full dark annealed state (A) to the saturated light-soaked state (B), this model predicts that the concentration of T_3^- centers is higher than that of the T_3^+ centers in the photodegraded material, and thus the density of the trapped carriers is much more important than that of the free carriers. Then the effect of the partial annealing treatment is to release electrons from the T_3^- centers and thus to reduce the density of trapped negative charges, which results in a shift of E_F towards the conduction band in order to maintain the charge neutrality of the material. Some metastable D^0-D^0 pairs might also release their trapped charges as a result of the partial annealing and become T_3^+-T_3^- charged pairs, which produces a decrease of the density of neutral dangling bonds. These phenomena explain very easily the C-T and ESR results obtained for all the samples when going from state B to state A_1 (state reached after the partial annealing).

The T_3^- center which has liberated its electron becomes a neutral T_p^0 site with a very small capture cross section. The T_p^0 center then has two possibilities during the long-time evolution of the film in the dark at room temperature: (i) either to recapture a localized electron with a small capture cross section and become again a negatively charged T_3^- center, which results in a backward shift of E_F towards the valence band; this should occur in samples where the defect relaxation is inhibited by the rigidity of the network, or (ii) to convert into a neutral $T_{sp^2}^0$ site and then capture a localized hole with a small capture cross section, in order to minimize its energy, giving a positively charged T_3^+ center which induces a further shift of E_F towards the conduction band; this situation should happen in unstrained material in which the defect relaxation is allowed by the surrounding amorphous network.

The first considered situation corresponds to the results obtained for the samples of series 3 deposited at the highest substrate temperature, which contain the lowest hydrogen concentration and in which the relaxation of the defects are consequently more difficult to occur because of the strained network. This makes the capture of a localized electron by the T_p^0 center more probable than its conversion into a $T_{sp^2}^0$ center. This is probably what happens during the long-time process in series 3.

The second situation corresponds to the results obtained for series 1 and 2 deposited at lower substrate temperature and thus exhibiting much higher hydrogen concentrations, which makes the defect relaxation much easier. In these series, the conversion of the T_p^0 center into a $T_{sp^2}^0$ center through a relaxation mechanism is more probable than in the preceding case, which results in an increase of the charged T_3^+ defect density after the $T_{sp^2}^0$ site has captured a localized hole. The relaxation mechanisms are expected to be easier in series 1, which exhibits the highest hydrogen concentration, than in series 2.

It is important to point out that the changes with time (i.e., the shift of E_F towards either the valence band or the conduction band observed after partial annealing), which strongly depend on the deposition temperature of the samples, lead us to eliminate any possibility that the motion (diffusion) of the hydrogen atoms may directly participate in this long-time process since it occurs at room temperature. However, the hydrogen should play an important role in these effects through the relaxation of the defects.

The conclusions of the present study do not weaken the importance of the Si-Si weak bond-breaking model[14,15,22] which is more commonly accepted. We only tried to show that our experimental results as a whole are more completely described by the charge distribution model,[23–25] which also has the advantage to take into account the existence in a-Si:H of other types of defects, namely, charged defects with a negative effective correlation ener-

gy, in addition to the traditional neutral dangling bonds. Consistent contentions by many workers that a spectrum of defects was possible in *a*-Si:H, in addition to traditional neutral dangling bonds, are now more widely admitted. This approach will certainly lead to a better understanding of the electronic and optical properties of the *a*-Si:H films, and more especially of the SW effect.

V. CONCLUSION

The present systematic study shows that the deposition conditions play an important role on the light-induced phenomena in *a*-Si:H. Moreover, a comparison between these results and those obtained in a previous study[30] indicates that, by changing one deposition parameter only (i.e., the rf power), the observed behavior of the samples upon illumination can be completely different. In particular, for the series deposited at the highest substrate temperature (250 °C) which exhibits the lowest hydrogen concentration, we obtain an "inverse" SW effect in the previous study,[30] while a "direct" SW effect is observed in the present case. Furthermore, this work confirms that more than one type of defect must be considered in order to completely describe our experimental results. According to our analysis, the neutral dangling bonds D^0 might initially coexist with charged T_3^+-T_3^- pairs, the respective proportions of these two types of defects depending on the deposition conditions.

ACKNOWLEDGMENT

We would like to thank Dr. D. Mencaraglia for diode preparations.

*Permanent address: Institut de Physique, Université d'Oran-es-Sénia, Algeria.

[1]D. L. Staebler and C. R. Wronski, Appl. Phys. Lett. **31**, 292 (1977).
[2]D. L. Staebler and C. R. Wronski, J. Appl. Phys. **51**, 3262 (1980).
[3]J. I. Pankove and J. E. Berkeyheiser, Appl. Phys. Lett. **37**, 705 (1980).
[4]I. Hirabayashi, K. Morigaki, and S. Nitta, Jpn. J. Appl. Phys. **19**, L357 (1980).
[5]H. Dersh, J. Stuke, and J. Beichler, Appl. Phys. Lett. **38**, 456 (1981).
[6]D. Jousse, P. Viktorovitch, L. Vieux-Rochaz, and A. Chenevas-Paul, J. Non-Cryst. Solids **35&36**, 767 (1980).
[7]M. Grunewald, K. Weber, W. Fuchs, and P. Thomas, J. Phys. (Paris) Colloq. **42**, C4-523 (1981).
[8]D. V. Lang, J. D. Cohen, J. P. Harbison, and A. M. Sergent, Appl. Phys. Lett. **40**, 474 (1982).
[9]J. L. Pankove, Solar Energy Mater. **8**, 141 (1982).
[10]N. M. Amer, A. Skumanich, and W. B. Jackson, Physica B **177&118**, 897 (1983).
[11]D. Han and H. Fritzsche, J. Non-Cryst. Solids **59&60**, 397 (1983).
[12]C. Lee, W. D. Ohlsen, P. C. Taylor, H. S. Ullal, and G. P. Ceasar, Phys. Rev. B **31**, 100 (1985).
[13]A. Skumanich, N. M. Amer, and W. B. Jackson, Phys. Rev. B **31**, 2263 (1985).
[14]M. Stutzmann, W. B. Jackson, and C. C. Tsai, Phys. Rev. B **32**, 23 (1985).
[15]M. Stutzmann, C. C. Tsai, and W. B. Jackson, Phys. Rev. B **34**, 63 (1986).
[16]R. A. Street, Appl. Phys. Lett. **42**, 597 (1983).
[17]I. Solomon, T. Dietl, and D. Kaplan, J. Phys. **39**, 1241 (1978).
[18]H. Fritzsche, Solar Energy Mater. **3**, 447 (1980).
[19]M. G. Mack and A. Madan, Appl. Phys. Lett. **41**, 272 (1982).
[20]H. Kakinuma, S. Nishukaw, and T. Watamabe, J. Non-Cryst. Solids **59&60**, 421 (1983).
[21]S. Kumar and S. C. Agarwal, Philos. Mag. B **49**, L53 (1984).
[22]M. Stutzmann, in *Proceedings of the Workshop on Physics and Applications of Amorphous Semiconductors, Torino, Italy,* edited by F. Danichelis (World Scientific, Singapore, 1988), p. 303.
[23]D. Adler, J. Phys. (Paris) Colloq. **42**, C4-3 (1981).
[24]D. Adler, Solar Cells **9**, 133 (1983).
[25]D. Adler, M. E. Eberhartt, K. H. Johnson, and S. A. Zygmunt, J. Non-Cryst. Solids **66**, 273 (1984).
[26]H. Labidi, K. Zellama, P. Germain, M. Astier, D. Lortigues, J. V. Bardeleben, M. L. Theye, L. Chahed, and C. Godet, Physica B **170**, 265 (1991).
[27]Qin Guo-Gang and Kong Guang-Lin, Philos. Mag. Lett. **57**, 117 (1988).
[28]W. B. Jackson, Phys. Rev. B **41**, 10257 (1990).
[29]W. B. Jackson and S. B. Zhang, Physica B **170**, 197 (1991).
[30]K. Zellama, H. Labidi, P. Germain, D. Lotrigues, L. Chahed, M. L. Theye, V. Desi, V. Coscia, G. Fameli, P. Memma, P. Roca, I. Cabarrocas, and C. Godet, Thin Solid Films **204**, 385 (1991).
[31]K. Zellama, J. D. Cohen, and T. Walsh, J. Non-Cryst. Solids **77&78**, 381 (1985).
[32]K. Zellama, J. D. Cohen, and J. P. Harbison, *Materials Issues in Applications of Amorphous Silicon Technology, San Francisco, 1985,* MRS Symposia Proceedings No. 49 (Materials Research Society, Pittsburgh, 1985), p. 311.
[33]J. D. Cohen, in *Semiconductors and Semimetals,* edited by J. I. Pankove (Academic, New York, 1984), Vol. 21, Pt. C, p. 9.
[34]K. Driss Khodja, A. Gheorghiu, and M. L. Theye, Opt. Commun. **55**, 169 (1985).
[35]N. M. Amer and W. B. Jackson, in *Semiconductors and Semimetals,* edited by J. I. Pankove (Academic, New York, 1984), Vol. 21, Pt. B, p. 83.
[36]R. C. Frye and D. Adler, Phys. Rev. B **24**, 5486 (1981).
[37]R. C. Frye and D. Adler, Phys. Rev. B **24**, 5812 (1981).
[38]J. D. Joannopoulos, D. Adler, and Bar Yam, in *Physics of Disordered Semiconductors,* edited by Kastner (Institute of Amorphous Studies, New York, 1985), p. 621.
[39]R. Meaudre, P. Jensen, and M. Meaudre, Phys. Rev. B **38**, 12449 (1988).
[40]R. A. Street, J. Kakolios, C. C. Tsai, and M. Hayes, Phys. Rev. B **35**, 1316 (1987).